Tellus SERIES A DYNAMIC METEOROLOGY AND OCEANOGRAPHY
PUBLISHED BY THE INTERNATIONAL METEOROLOGICAL INSTITUTE IN STOCKHOLM

Modelling economic losses of historic and present-day high-impact winter windstorms in Switzerland

By CHRISTOPH WELKER[1]*†, OLIVIA MARTIUS[1], PETER STUCKI[1], DAVID BRESCH[2], SILKE DIERER[3] and STEFAN BRÖNNIMANN[1], [1]*Oeschger Centre for Climate Change Research and Institute of Geography, University of Bern, Bern, Switzerland*; [2]*Swiss Reinsurance Company, Zurich, Switzerland*; [3]*METEOTEST, Bern, Switzerland*

(Manuscript received 27 August 2015; in final form 1 March 2016)

ABSTRACT

This study investigates the wind gusts and associated economic loss patterns of high-impact winter windstorms in Switzerland between 1871 and 2011. A novel approach for simulating windstorm-related gusts and losses at regional to local scales is applied to a sample of 84 windstorms. The approach involves the dynamical downscaling of the Twentieth Century Reanalysis (20CR) ensemble mean to 3-km horizontal grid size using the Weather Research and Forecasting (WRF) model. Economic losses are simulated at municipal level for present-day asset distribution based on the downscaled (parameterised) wind gusts at high spatiotemporal resolution using the open-source impact model climada. A comparison with insurance loss data for two recent windstorms ("Lothar" in 1999, "Joachim" in 2011) indicates that the loss simulation allows to realistically simulate the spatial patterns of windstorm losses. The loss amplitude is strongly underestimated for 'Lothar', while it is in reasonable agreement for 'Joachim'. Possible reasons are discussed. Uncertainties concerning the loss simulation arise from the wind gust estimation method applied; estimates can differ considerably among the different methods, in particular over high orography. Furthermore, the quality of the loss simulation is affected by the underlying simplified assumptions regarding the distribution of assets and their susceptibilities to damage. For the whole windstorm sample, composite averages of simulated wind gust speed and loss are computed. Both composites reveal high values for the densely populated Swiss Plateau and lower values for south-eastern Switzerland; metropolitan areas stand out in the loss composite. Eight of the top 10 events concerning the losses simulated for present-day asset distribution and summed over all Swiss municipalities occurred after 1950. It remains uncertain whether this is due to decadal-scale changes of winter windstorms in Switzerland or merely due to a possible bias of the 20CR ensemble mean towards lower wind speeds in the period before around 1950.

Keywords: mid-latitude winter storms, impact modelling, risk assessment, 20CR, WRF, dynamical downscaling, wind gust estimation

To access the supplementary material to this article, please see Supplementary files under 'Article Tools'.

1. Introduction

Extreme windstorms are among the most destructive meteorological hazards affecting Switzerland (Imhof, 2011). Their socio-economic impacts depend on the severity of the windstorms and also on the exposure and vulnerability of the values at risk (IPCC, 2012). Natural hazard risks always involve the combination of the hazard and socio-economic factors, and both are subject to changes over time (e.g. Keiler et al., 2006). The assessment of windstorm-related risks is important for insurance and reinsurance companies and also for local governments, which are responsible for identifying measures to minimise the impact from natural hazards at the lowest cost to society (e.g. ECAWG, 2009).

Good estimates of the probability of occurrence are indispensable for assessing windstorm risks. To study the regional impacts of windstorms, a large sample of events is needed for

*Corresponding author.
email: christoph.welker@gvz.ch
†Now at: GVZ Gebäudeversicherung Kanton Zürich, Thurgauerstrasse 56, CH-8050 Zürich, Switzerland.

Citation: Tellus A 2016, **68**, 29546, http://dx.doi.org/10.3402/tellusa.v68.29546

which quantitative meteorological data and ideally loss data at high spatiotemporal resolution are available (e.g. Haas and Pinto, 2012). However, extreme windstorms are rare by definition and the limited length of the observations is an important constraint in the analysis of extreme weather events (Frei and Schär, 2001). In general, the observational records of windstorm events are not satisfactory when used to estimate the probability of occurrence of the most extreme events because atmospheric data from observations usually span relatively short periods, have coarse spatiotemporal resolution, and often suffer from inhomogeneities (Della-Marta et al., 2010). Similar problems apply to reanalysis data, which are based on atmospheric observations and dynamical atmospheric models. To increase the sample of windstorms and related wind fields, insurance and reinsurance companies often combine meteorological data with artificial windstorm events generated by stochastic models and dynamical atmospheric models. However, dynamical models also have their limitations; they have biases related to their numerics and physics parameterisations and often coarse spatiotemporal resolution (Della-Marta et al., 2010).

In Switzerland, the information on historic windstorms is overall sparse and incomplete (Stucki et al., 2014). The available historic weather and loss reports are generally descriptive and do not provide quantitative information. However, government regulations increasingly ask insurances for protecting their balance sheets up to losses with estimated return periods of 200 yr or more (Haylock, 2011) and building norms are tied to certain return periods. The Twentieth Century Reanalysis (20CR) version V2 ensemble dataset (Compo et al., 2011) currently spanning 1871–2012 offers a valuable basis for a quantitative windstorm risk assessment. The assessment period is extended compared to the period that was available until recently with the approximately 60 yr of global atmospheric reanalysis data.

The large-scale atmospheric flow conditions associated with windstorms in Switzerland are overall well represented in the 20CR (e.g. Stucki et al., 2015). However, the horizontal grid spacing of the 20CR (2° by 2°) is too coarse to realistically represent the complex orography of Switzerland. This affects the representation of smaller-scale features of the wind field influenced by the local orography. Brönnimann et al. (2012) showed that the 20CR has deficiencies in adequately representing regional to local-scale atmospheric conditions using the example of a hazardous foehn storm in Switzerland in January 1919. This shortcoming can be overcome by applying downscaling methods. Previous studies quantifying the impacts of European windstorms on regional scales combined relatively coarse-resolution, large-scale atmospheric data from reanalyses (or general circulation models) with regional climate models resulting in high-resolution simulations of the surface wind field over the regions of interest (typically with horizontal grid sizes of 5–50 km; e.g. Della-Marta et al., 2010; Schwierz et al., 2010).

Using the 20CR as a starting point, this study illustrates a method to simulate the wind gust speeds and related economic impact of both historic and present high-impact winter windstorms in Switzerland. The selection of windstorms is based on a catalogue of high-impact windstorms in Switzerland since 1859 (Stucki et al., 2014). Our method involves the dynamical downscaling of the 20CR ensemble mean to a 3-km horizontal grid size using the Weather Research and Forecasting (WRF) model (Skamarock et al., 2008) and the subsequent loss simulation using the winter windstorm damage assessment module of the open-source climada natural catastrophe loss model (denoted climada model in the following; Bresch, 2014). This loss modelling chain was used by Stucki et al. (2015) to simulate a hazardous foehn storm in Switzerland in February 1925. The simulated loss pattern for this specific windstorm looks realistic compared to historic loss information, showing the potential of the method to realistically simulate the impacts of windstorm events in Switzerland.

This study aims at presenting the potentials and limitations of the loss modelling technique introduced by Stucki et al. (2015), using the example of the very intense windstorm 'Lothar' on 26 December 1999 (e.g. Wernli et al., 2002) that caused major damage across Switzerland and the recent windstorm 'Joachim' on 17 December 2011. More specifically, for both windstorm events we ask the following questions: how well is the spatial pattern of windstorm losses simulated, and how well the loss amplitude? And in general, what is necessary to accomplish a good simulation of windstorm losses? To answer these questions, we compare the simulated windstorm losses with proprietary insurance loss data and the downscaled wind gust speeds used for the loss simulation with instrumental wind gust measurements. The loss modelling technique is then applied to more than 80 historic and present high-impact winter windstorms in Switzerland, providing information about the typical wind gust and loss patterns.

2. Data and methods

Our selection of winter windstorm events is based on a catalogue of high-impact windstorms in Switzerland since the middle of the 19th century described in Stucki et al. (2014). We considered the strongest winter windstorms in this catalogue between 1871 and 2011, that is, in total 84 high-impact windstorms in Switzerland during the winter months October through March (see Supplementary Table A1).

Our windstorm sample involves the two main groups of windstorms affecting Switzerland: westerly windstorms and foehn storms (e.g. Jungo et al., 2002). Typically, westerly

windstorms are associated with deep extratropical low-pressure systems forming over the North Atlantic (e.g. Welker and Martius, 2015). They are characterised by high wind speeds from mainly westerly directions and in most cases affect regions north of the Alps and high Alpine regions. Foehn storms are normally characterised by mainly southerly (northerly) winds that affect north–south oriented Alpine valleys and the northern (southern) Alpine forelands (e.g. Richner and Hächler, 2013).

High-resolution surface winds (10 m above ground) over Switzerland for the 84 windstorms were obtained by performing a three-step dynamical downscaling of the 20CR ensemble mean using the WRF model (see also Brönnimann et al., 2014; Stucki et al., 2015). The horizontal grid size decreases from 45 km in downscaling domain 1 (25°N–66°N, 34°W–49°E), to 9 km in domain 2 (43°N–53°N, 1°E–14°E), and to 3 km in domain 3 (46°N–48°N, 6°E–11°E). The innermost domain includes Switzerland and parts of the neighbouring countries. The WRF model was run with 31 vertical layers and the simulations were started 18 hours before each windstorm period and were ended 18 hours after the windstorm period.

A realistic simulation of orographic wind systems in Switzerland depends on a realistic representation of the orography in the WRF model (see also Stucki et al., 2015). Figure 1 shows orography as represented in the WRF model: well-known north–south oriented foehn valleys, such as sections of the Rhine Valley in eastern Switzerland

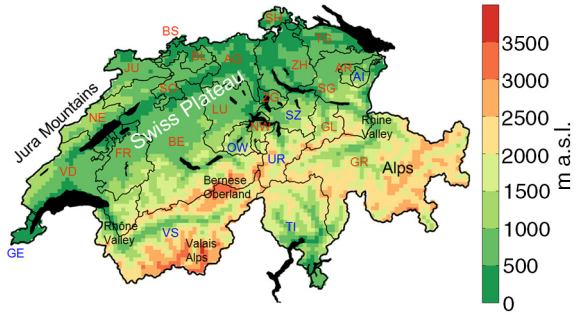

Fig. 1. WRF terrain height of the innermost model domain in m a.s.l. (colour scheme; horizontal grid size of 3 km). Places mentioned in the text, main regions of Switzerland (i.e. Jura Mountains, Swiss Plateau, and Alps), lakes, and cantonal boundaries are indicated. Two-letter abbreviations of the GUSTAVO cantons are given in blue letters [Geneva (GE), Uri (UR), Schwyz (SZ), Ticino (TI), Appenzell-Innerrhoden (AI), Valais (VS), Obwalden (OW)] and of the remaining cantons in red letters [non-GUSTAVO cantons; Aargau (AG), Appenzell-Ausserrhoden (AR), Bern (BE), Basel-Country (BL), Basel-City (BS), Fribourg (FR), Glarus (GL), Grisons (GR), Jura (JU), Lucerne (LU), Neuchâtel (NE), Nidwalden (NW), St. Gallen (SG), Schaffhausen (SH), Solothurn (SO), Thurgau (TG), Vaud (VD), Zug (ZG), Zurich (ZH)].

or of the Rhône Valley in western Switzerland, are captured. Nonetheless, the representation of Switzerland's complex orography is relatively smooth due to the still coarse 3-km horizontal grid size.

Because wind damage is typically related to high wind gust speeds (e.g. Klawa and Ulbrich, 2003), the WRF post-process diagnostic of wind gusts (denoted WPD) was used for impact modelling. This estimation of wind gust speeds at 10-m height (WGS_{10m}) takes into account both the wind speed at 10-m height (WS_{10m}) and the wind speed at the top of the planetary boundary layer [WS_{PBL}, h_{PBL}; eq. (1)]:

$$WGS_{10m} = WS_{10m} + (WS_{PBL} - WS_{10m}) * \left(1 - \frac{h_{PBL}}{2000m}\right) \quad (1)$$

Deep planetary boundary layers (>1000 m) are reduced to a height of 1000 m above the ground, so that the term $h_{PBL}/2000\ m$ reaches values of 0.5 at most. In this study, a wind gust footprint is defined as the maximum downscaled surface wind gust speed at each grid point in the innermost model domain during a windstorm event.

To estimate the uncertainty due to the wind gust estimation method, we additionally calculated surface wind gust speeds using the German Weather Service approach implemented in the COSMO Climate Local Model (denoted COS method; Schulz and Heise, 2003; Schulz, 2008). The COS method derives the maximum turbulent 10-m wind gusts using the wind speed at 10 m above the ground and an empirical relation with the friction velocity [u_*; eqs. (2) and (3)]:

$$WGS_{10m} = WS_{10m} + 3 \cdot 2.4 \cdot u_* \quad (2)$$

$$u_* = WS_{10m} * \sqrt{C_d} \quad (3)$$

C_d is the drag coefficient. The COS method emphasises the local orography and is thus complementary to the WPD method which takes into account the surface wind speed and also the wind speed at the top of the planetary boundary layer.

For the two windstorms 'Lothar' and 'Joachim', instrumental wind gust speed measurements from the SwissMetNet (SMN) dataset, operated by the Federal Office of Meteorology and Climatology MeteoSwiss and available for the period since 1981, were used for evaluation of the estimated surface wind gust speeds. Suitable wind gust speed measurements for this evaluation are available at 63 measuring stations which are spread all over Switzerland. Based on the documentation available for each station, these stations were classified into mountain stations, stations in valleys, and stations located in flat terrain (see Stucki et al., 2016). The flat terrain stations are almost exclusively located in the densely populated Swiss Plateau situated in between the Jura Mountains and the Alps.

For each of the 84 windstorm events, economic losses were simulated at municipal level for present-day asset distribution using the climada model (Bresch, 2014). The climada model calculates losses to buildings and their content due to extratropical and tropical storms and was successfully applied in earlier studies (e.g. Della-Marta et al., 2010; Schwierz et al., 2010; Raible et al., 2012; Reguero et al., 2014; Stucki et al., 2015). The model is documented in detail in the climada manual (see Bresch, 2014). The complexity of the model is reduced compared to state-of-the-art loss models operationally in use in the insurance industry. We consider this an advantage because the reduced complexity allows us to accomplish a well interpretable assessment of the model skill.

We prescribed the year-2009 population distribution at municipal level in the climada model, assuming assets of 250 000 CHF per inhabitant (Fig. 2). For each municipality i, the monetary loss was simulated based on the product between the asset value and a vulnerability term [eq. (4)]:

$$\frac{Loss_i}{Area_i} = \frac{Asset_i \cdot MDD\left(WGS_{10m,i}\right) \cdot PAA\left(WGS_{10m,i}\right)}{Area_i} \quad (4)$$

This vulnerability term is defined as the product between a factor quantifying the mean damage degree (MDD) ranging from 0 to 1 (i.e. from no to total destruction) and a factor indicating the percentage of assets affected (PAA) ranging from 0 to 1 (i.e. from none affected to all affected). The MDD and PAA factors were derived by Schwierz et al. (2010) based on movable property and building losses associated with European winter windstorms. Both MDD and PAA are non-linear functions of the maximum wind gust speed during a windstorm event (Fig. 3).

The climada model relates the damage of a particular asset to the incurring wind gust at this particular location, that is, the respective municipality. More precisely, the maximum surface wind gust speed at each grid point during the respective windstorm event was linked to the centroids of the Swiss municipalities by using a triangulation-based linear interpolation method. The interpolated wind gust speeds at municipal level were then used for the simulation of windstorm losses.

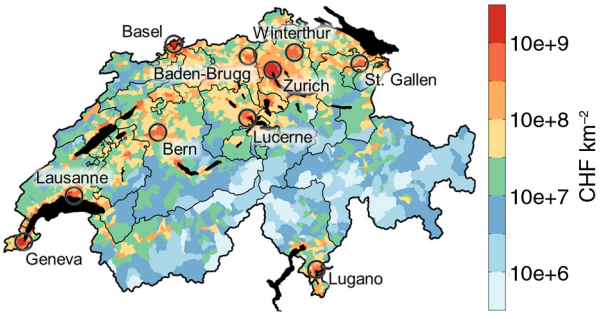

Fig. 2. Assets in CHF per km^2 at municipal level for year-2009 asset distribution (colour scheme; base 10 logarithmic scale) as prescribed in the climada model (i.e. number of inhabitants in 2009 multiplied by 250 000 CHF). Circles indicate the 10 major agglomerations of Switzerland on 1 January 2009 (according to the Swiss Federal Statistical Office). Cantonal boundaries and lakes are outlined.

The monetary loss simulated for a particular municipality was further divided by the area of the municipality to allow for visual comparability of the losses simulated for municipalities with differing areas; and also to allow for comparability with insurance loss data available at postal code and cantonal levels (see below). The division by the municipal area has the effect that urban areas are emphasised compared to rural areas because urban areas are densely populated but the corresponding municipal areas are generally small. Nevertheless, the linear relationship between the population (and thus the asset value) of a municipality and the municipal area is very weak for the considered 2624 Swiss municipalities ($R = 0.09$), pointing to a more complex relationship between the population and the area of Swiss municipalities.

For 'Lothar' and 'Joachim', we compared simulated losses with insurance loss data, that is, movable property and building loss data at postal code level provided by the Swiss Mobiliar (MOB) and building loss data at cantonal level provided by the Intercantonal Reinsurance (IRV). In Switzerland, MOB is the largest private insurer against property loss and the largest insurance provider against damage to buildings in the seven Swiss cantons of Geneva, Uri, Schwyz, Ticino, Appenzell-Innerrhoden, Valais, and Obwalden – known as the GUSTAVO cantons (see Fig. 1). IRV is the reinsurance association of the 19 cantonal building insurances. A peculiarity of the Swiss insurance system is that in the GUSTAVO cantons damage to buildings is insured by private insurance companies such as MOB only, whereas cantonal building insurances insure damage to buildings in the remaining 19 cantons (denoted non-GUSTAVO cantons in the following). The available MOB data do not comprise deductibles, which amount to approximately 500 CHF (1000 CHF) per insured movable property (building); each of the cantonal building insurances, in turn, has its own regulations for deductibles (see Imhof, 2011). Furthermore, neither MOB nor IRV data were normalised to present-day exposure levels.

It is important to emphasise that we do not simulate building losses (as in case of the IRV data) with our loss modelling technique, but rather a combination of movable property and building losses (as in case of the MOB data). As a consequence, a full comparison between our loss simulations and the insurance loss data is not possible with the available data. Furthermore, a full evaluation of our loss modelling approach is complicated by the characteristics

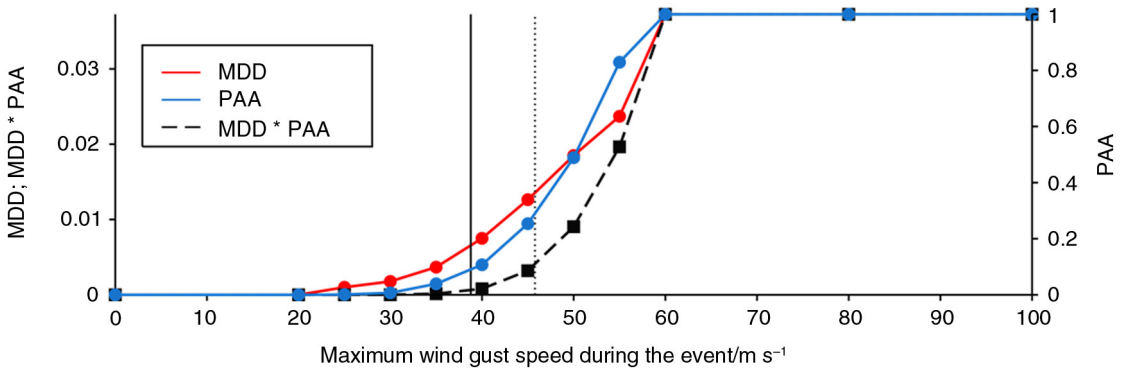

Fig. 3. Mean damage degree (red; left y-axis), percentage of assets affected (blue; right y-axis), and product of *MDD* and *PAA* (black; left y-axis) as a function of maximum wind gust speed during the windstorm event. A linear interpolation was applied between two consecutive points (denoted with a straight line segment). The maximum downscaled surface wind gust speed over Switzerland during 'Lothar' (added with 7 m s^{-1}; i.e. the average bias of estimated surface wind gust speeds using the WPD method compared to instrumental wind gust speed measurements in case of 'Lothar'; see Table 1) is marked by the solid (dotted) vertical line.

of the available insurance data: (i) the insurance loss data are available at different spatial levels (postal code and cantonal level) which is problematic for the comparison of the spatial patterns of the losses, (ii) by the building insurance system in the GUSTAVO vs. non-GUSTAVO cantons (see above), and (iii) not publicly available information about, for example, market share in case of data from the private insurance company MOB. Furthermore, the insurance data are not normalised to present-day exposure levels. All these difficulties and limitations have to be considered in the comparison between simulated and insured windstorm losses in Section 3.3. Nevertheless, the building loss data at cantonal level provided by the IRV are our 'best guess' for the losses in the non-GUSTAVO cantons. Accordingly, the movable property and building loss data at postal code level of the MOB are our 'best guess' for the losses in the GUSTAVO cantons.

For further evaluation of our loss modelling technique, we performed, for windstorms 'Lothar' and 'Joachim', independent loss simulations on the basis of real MOB insurance portfolios at postal code level. These loss simulations were based on wind gust estimates from the operational versions of the COSMO model at MeteoSwiss, that is, COSMO-7 for 'Lothar' (horizontal grid size of 7 km) and COSMO-2 for 'Joachim' (horizontal grid size of 2 km), using the COS wind gust estimation method [denoted COSMO/COS hereafter; note that in the MeteoSwiss estimation of wind gusts at 10 m above the ground the mean wind at 30 m above the ground was used in eq. (2) instead of WS_{10m}]. Furthermore, the simulations differ from the loss simulations presented before in the following points: the geographical location of each postal code's main settlement was used in the spatial association of hazard intensity to asset (instead of the geographical centroid) and a distinction between movable properties and buildings was made.

3. Case studies

In this section, we present our approach in more detail using the examples of windstorms 'Lothar' and 'Joachim'.

3.1. *Downscaled surface wind gusts*

The first step of our approach is the dynamical downscaling of the 20CR ensemble mean using the atmospheric model WRF and subsequent wind gust estimation using the WPD method. In this way, surface wind gust speeds over Switzerland at high spatiotemporal resolution were obtained that were subsequently used for the simulation of windstorm losses (Section 3.2).

The loss amount associated with a windstorm event depends on both its intensity (here, maximum surface wind gust speed during the event) and its track (Schwierz et al., 2010). A correct simulation of the track is important because the windstorm could either affect a densely populated region and cause large damage or could pass over a sparsely populated region and cause little damage. Furthermore, due to a non-linear relationship between wind gust speeds and inflicted damages, small changes in wind gust speed may lead to substantial changes in damages (see also Watson and Johnson, 2004). Therefore, it is crucial that both the track and wind gust speeds of the windstorm are simulated as accurately as possible for a realistic simulation of windstorm losses.

Figure 4a shows the 20CR ensemble mean surface wind speed for the North Atlantic and European sectors on 26 December 1999, 12 UTC, that is, at the time when surface winds were highest over Switzerland during 'Lothar'. High surface winds over Switzerland associated with 'Lothar' are not realistically captured in the 20CR, due to its coarse 2° by 2° latitude-longitude grid and associated unrealistic

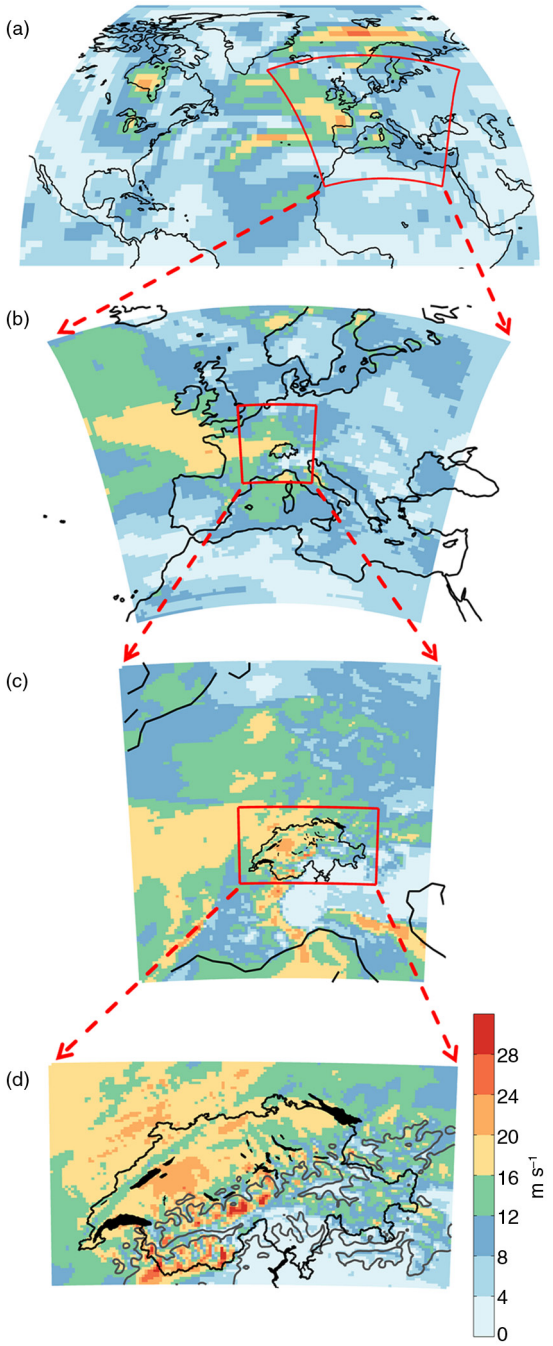

Fig. 4. (a) 20CR ensemble mean surface wind speed in m s^{-1} (2° by 2° latitude–longitude grid) at the time of windstorm 'Lothar' on 26 December 1999, 12 UTC. The red box indicates domain 1 (25°N–66°N, 34°W–49°E) of the applied stepwise dynamical downscaling of the 20CR ensemble mean using WRF. (b–d) Analogous to (a), but shown are the downscaled surface wind speeds in m s^{-1} for downscaling domain 1, domain 2 (43°N–53°N, 1°E–14°E), and domain 3 (46°N–48°N, 6°E–11°E); grid sizes of 45 km, 9 km, and 3 km. The border of Switzerland and Swiss lakes are marked. The grey contours in (d) show the 1500 m a.s.l. WRF terrain height.

representation of Switzerland's complex orography. In the high-resolution simulation (3-km horizontal grid size), smaller-scale features of the surface wind field such as high wind speeds over the Swiss Plateau and the Alps are clearly recognisable (Fig. 4d).

Figure 5 shows the wind gust footprints for the two windstorms 'Lothar' and 'Joachim'. Compared to instrumental wind gust speed measurements, estimated surface wind gusts are overall too low in case of 'Lothar' and much better simulated in case of 'Joachim' (Table 1). For all measuring stations, a negative bias of 7.0 m s^{-1} is found on average for 'Lothar' and a positive bias of 0.2 m s^{-1} is found on average for 'Joachim'. These numbers indicate that the wind gust footprint of some windstorms is easier to simulate than that of others.

3.2. *Simulation of windstorm-related economic losses*

Based on the wind gust footprints for 'Lothar' and 'Joachim' (Fig. 5), windstorm-related losses were simulated at municipal

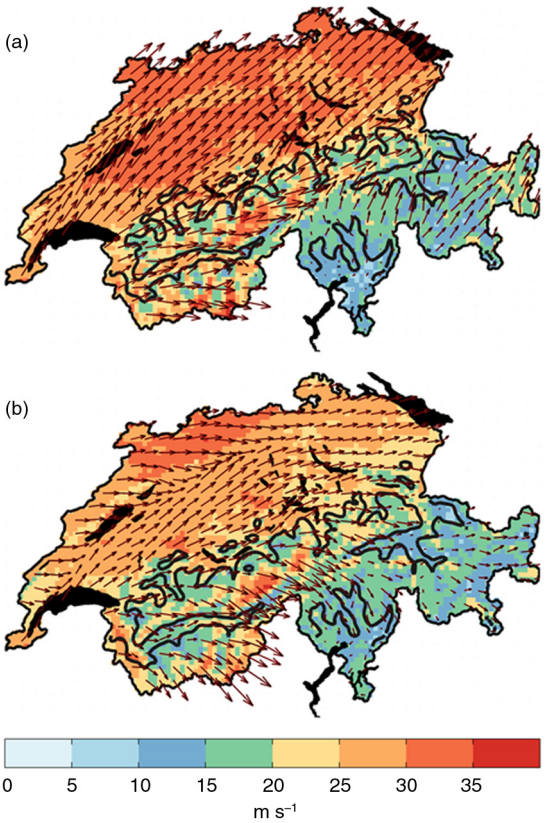

Fig. 5. Wind gust footprints for (a) 'Lothar' and (b) 'Joachim' in m s^{-1} (colour scheme). Vectors indicate both direction and magnitude of the surface wind at the times when wind gust speeds were maximal in Switzerland. The WRF terrain height 1500 m a.s.l. contour line and lakes are outlined.

Table 1. Average bias of estimated surface wind gust speeds using the WPD method (COS method) compared to instrumental wind gust speed measurements from the SMN dataset in m s^{-1} (i.e. estimated wind gusts minus measured gusts) for windstorms 'Lothar' and 'Joachim'

		Average wind gust speed bias in m s^{-1}			
Windstorm event	Wind gust estimation	Mountain stations	Stations in valleys	Stations in flat terrain	All stations
'Lothar'	WPD	−17.0	−2.5	−5.8	−7.0
	COS	−18.4	−6.0	−7.6	−9.3
'Joachim'	WPD	−5.4	3.7	0.2	0.2
	COS	−4.2	2.5	−0.2	−0.1

Measuring stations were classified into mountain stations, stations in valleys, and stations in flat terrain.

level for present-day asset distribution using the climada model. Regarding the spatial distribution, the simulated losses for 'Lothar' show high values for almost the entire Swiss Plateau and low values for south-eastern Switzerland (Fig. 6a). Metropolitan areas are clearly recognisable which demonstrates that simulated windstorm losses depend on the severity of the windstorm (i.e. hazardous wind gust speeds; Fig. 5a) and also on the exposure and vulnerability of the values at risk (see Figs. 2 and 3). The simulated losses are overall lower in case of 'Joachim' (Fig. 7a).

'Lothar' was truly exceptional in the past approximately 140 yr concerning its impact: in terms of simulated losses summed over all Swiss municipalities, 'Lothar' ranks first of all 84 windstorm events and 'Joachim' ranks 8th (see Supplementary Table A1). Simulated windstorm losses for 'Lothar' and 'Joachim' are compared with insurance loss data in the following section.

3.3. *Comparison with insurance loss data*

The comparison of simulated losses with insurance loss data for 'Lothar' is shown in Fig. 6. To allow for visual comparability, both simulated losses and insured losses were normalised with the corresponding municipal area, postal code area and cantonal area. Because the insurance loss data are proprietary, both simulated and insured losses were classified into loss categories (ranging from low to high losses; base 10 logarithmic scale) and the same colour scheme was used for both datasets. Figure 6b and c show for 'Lothar' movable property and building loss data at postal code level provided by the MOB and building loss data at cantonal level provided by the IRV. According to the IRV data, the highest losses per km^2 occurred in the cantons of Basel-City, Zug, Nidwalden, Basel-Country, and Aargau (cantons marked in Fig. 6c), whereas the lowest losses per km^2 occurred in the canton of Grisons (for locations see also Fig. 1). The comparison of the IRV loss data with our loss simulation is complicated by the different spatial resolutions of the data (cantonal vs. municipal level); for example, a large proportion of the assets in the canton of Vaud is located along Lake Geneva (Fig. 2), which is not discernible in the cantonal IRV data (Fig. 6c). Nevertheless, the comparison indicates that the spatial pattern of losses is overall well simulated. This spatial information on the loss pattern is of use to a range of end-users involved in the assessment of windstorm-related risks.

Concerning the amplitude of the simulated losses, the comparison of simulated losses with insurance loss data reveals that the loss amplitude is on average strongly underestimated: the IRV loss added up is 17 times as high as the simulated loss summed over all municipalities in the non-GUSTAVO cantons. The loss amplitude is strongly underestimated in the GUSTAVO cantons as well: the MOB loss summed over all postal codes situated in the GUSTAVO cantons is almost 15 times as high as the simulated loss summed over all municipalities in the GUSTAVO cantons.

There are several possible reasons for the considerable underestimation of the loss amplitude in case of 'Lothar'. First, assuming assets of 250 000 CHF per inhabitant in the climada model is an oversimplification and a more realistic distribution of values at risk as well as of their susceptibilities to damage would lead to a more realistic loss simulation. At least for 'Lothar', we however consider the effect of our simplified assumption regarding the asset distribution to be rather small: simulating losses on the basis of MOB insured values does not improve the loss simulation (Table 2). Second, the downscaled surface wind gust speeds for 'Lothar' are systematically lower than the measurements. We find a negative bias over the Swiss Plateau of 5.8 m s^{-1} on average (Table 1). For the whole of Switzerland, the negative bias is 7 m s^{-1} on average. To examine the effect of this underestimation of the wind gusts on our loss estimation, we increased the maximum wind gust speed during 'Lothar' by +7 m s^{-1} at every grid point located in Switzerland before performing the loss modelling. With these changes, the simulated losses are very similar to the IRV losses: the IRV loss added up is 4 % lower than the simulated loss summed over all municipalities in the non-GUSTAVO cantons (compared to 17 times as high in case of no change). This experiment also indicates that biases

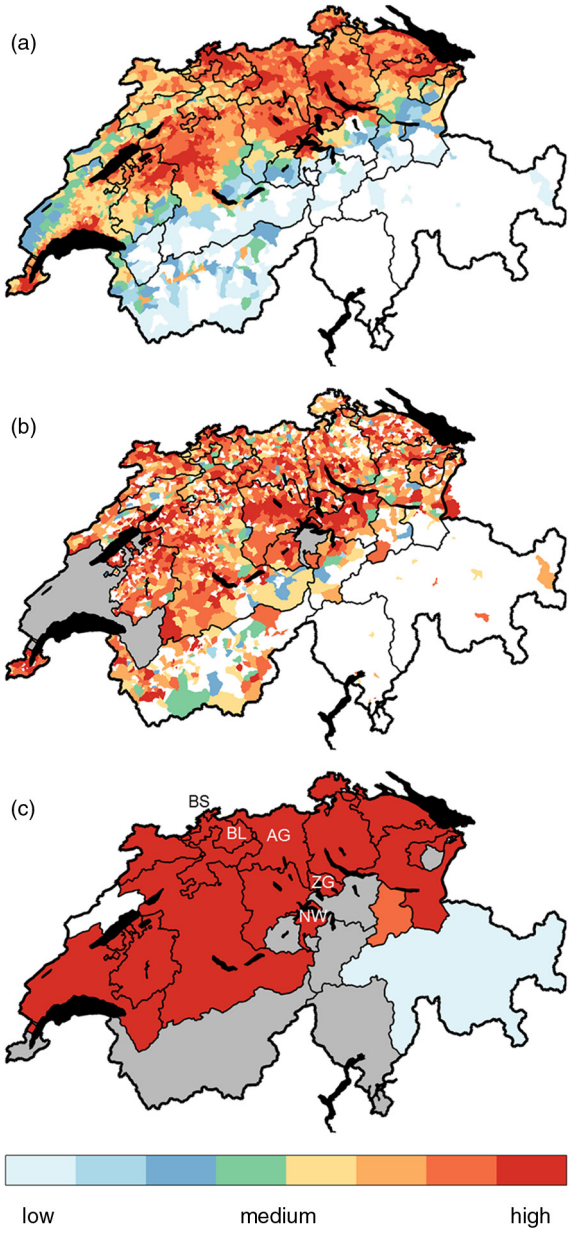

Fig. 6. (a) Simulated loss per km^2 at municipal level for 'Lothar' under year-2009 asset distribution. (b, c) Insured loss per km^2 for 'Lothar': (b) the sum of MOB movable property and building loss data at postal code level and (c) building loss data at cantonal level provided by the IRV. MOB is not allowed to insure damage to movable properties and buildings in the cantons of Vaud and Nidwalden [marked grey in (b)]. Grey cantons in (c) are not covered by the IRV (GUSTAVO cantons), no damage information is available for the canton of Neuchâtel (white), and the cantons with the highest losses per km^2 are marked because loss maxima are not discernible. Note that the same colour scheme (base 10 logarithmic scale) was used for simulated losses as well as insured losses in this study. The loss data were classified into loss categories (ranging from low to high losses) because the insurance loss data are proprietary. Cantonal boundaries and lakes are outlined.

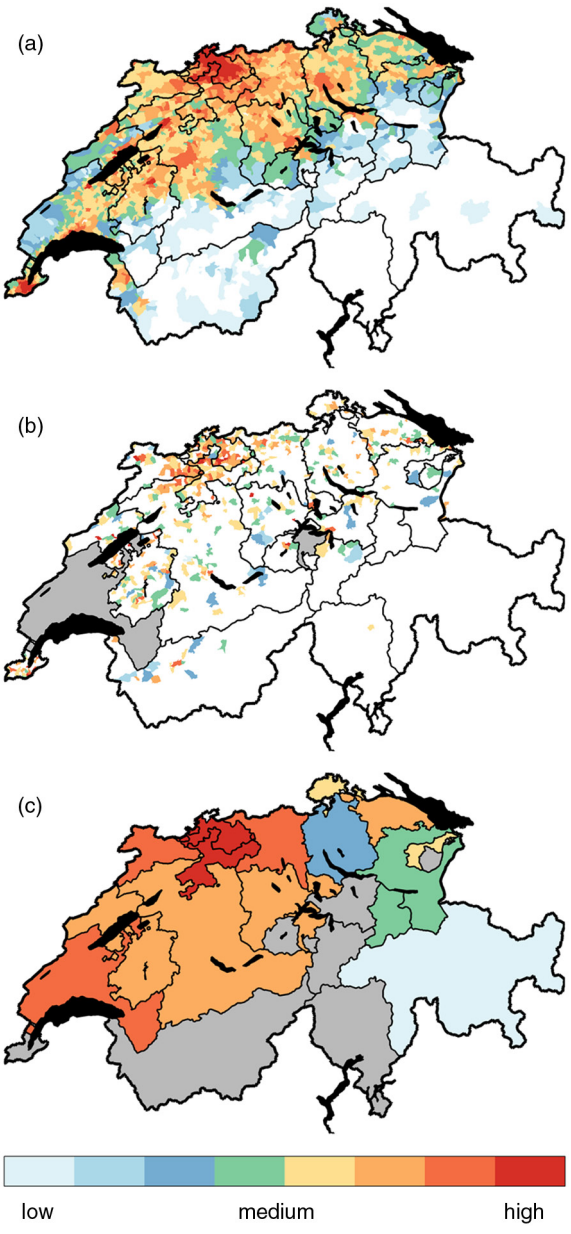

Fig. 7. The same as Fig. 6, but for windstorm 'Joachim'.

in wind gust speed are most relevant for the loss simulation in case of the strongest windstorm events, due to the non-linear damage function applied (shown schematically for 'Lothar' in Fig. 3).

For 'Joachim', the agreement between the spatial loss patterns from our simulation and from insurance loss data is very good (Fig. 7). For example, the loss maximum in the cantons of Basel-City, Basel-Country, and Solothurn, found in the IRV data as well as in the MOB data, is very well captured in our loss simulation.

The IRV loss added up is more than three times as high as the simulated loss summed over all municipalities in the

Table 2. Ratio of MOB insured losses to losses simulated based on MOB insurance portfolios at postal code level (here, distinction made between movable properties and buildings) for 'Lothar' and 'Joachim'

Windstorm event	Wind gust estimation	Movable property losses	Building losses
'Lothar'	WPD	13.7	59.4
	COS	8.9	22.6
	COSMO/COS	1.1	1.4
'Joachim'	WPD	1.6	2.9
	COS	0.2	0.3
	COSMO/COS	0.5	0.6

Loss simulations were performed on the basis of wind gust estimates from the operational versions of the MeteoSwiss COSMO model using the COS wind gust estimation method (COSMO/COS) as well as from dynamical downscaling of the 20CR ensemble mean using WRF and applying the WPD and COS wind gust estimation methods.

non-GUSTAVO cantons. Thus, the amplitude of the simulated losses is on average underestimated, however less pronounced as in case of 'Lothar'. The MOB loss summed over all postal codes in the GUSTAVO cantons is approximately 40 % of the simulated loss summed over all municipalities in the GUSTAVO cantons. For 'Joachim', the agreement of the downscaled surface wind gust speeds over the Swiss Plateau with the instrumental wind gust speed measurements is on average much better than in case of 'Lothar', with a positive bias of only 0.2 m s^{-1} on average (Table 1). Subtracting this bias from the wind gust footprint for 'Joachim' does not result in an improvement of the simulation concerning the loss amplitude for the non-GUSTAVO cantons, but leads to a slight improvement for the GUSTAVO cantons (i.e. improvement by four percentage points).

Table 2 indicates that, in case of 'Lothar', the simulation of the loss amplitude is considerably improved if it is based on the MeteoSwiss COSMO/COS data, emphasising the importance of an accurate estimation of the wind gust footprint for the loss simulation. Latter finding applies in particular to the strongest windstorm events. The effect is weaker for 'Joachim' (Table 2).

For 14 high-impact winter windstorms in Switzerland between 1993 and 2011 including 'Lothar' and 'Joachim', Stucki et al. (2016) calculated average biases of wind gust speed estimates (estimated using the WPD method) compared to instrumental wind gust speed measurements at 63 stations in Switzerland from the SMN dataset (all of these 14 windstorms are also included in our sample of 84 windstorms). They found an average bias of -6.9 m s^{-1} for mountain stations, 2.1 m s^{-1} for stations in valleys, -1.8 m s^{-1} for stations in flat terrain, and -1.5 m s^{-1} for all stations. These numbers indicate that for mountain and flat terrain locations the wind gust estimates for 'Lothar' (Table 1) are considerably worse than the average for the 14 windstorms. In contrast, the estimates for 'Joachim' are better than the average (except for valley locations). We infer that the strong underestimation of the wind gust speeds in case of 'Lothar' is not necessarily representative for the other windstorm events in our sample, which leads us to analyse the wind gusts and associated loss patterns of all 84 windstorms in the following section.

4. Analysis of 84 windstorm events

To provide information about the typical wind gust and loss patterns of hazardous windstorms in Switzerland, we performed the computations described before for all 84 high-impact winter windstorms in Switzerland. Recently, a similar sample of windstorm events was used to generate a wind hazard map for Switzerland applying the same downscaling method as presented in this study and estimating wind gust speeds concerning different return periods (for more details refer FOEN, 2015).

Figure 8a shows the composite mean wind gust speed for the 84 windstorm events. Wind gust speeds were higher on average on the north side of the Alps, over the Jura Mountains and Swiss Plateau, than over south-eastern Switzerland; only few windstorms in our sample heavily affected south-eastern Switzerland. The highest values are found over high mountain regions like the Bernese Oberland and the Valais Alps. The wind gusts in north–south oriented foehn valleys such as the Rhine Valley or Rhône Valley are relatively low in the composite mean (Fig. 8a). They are considerably higher in the composite maximum (not shown). Indeed, the variability among the 84 windstorms is largest in the foehn valleys (Fig. 8b).

In accordance with the wind gust composite (Fig. 8a), the composite mean of simulated loss at municipal level shows high values for the north side of the Alps, in particular for the densely populated Swiss Plateau, and lower values for south-eastern Switzerland (Fig. 9a). Major metropolitan areas, such as Geneva, Lausanne, Bern, Basel, or Zurich (for locations see Fig. 2) are clearly recognisable in the loss composite mean. As a result of typically high wind gust speeds over high mountain regions (Fig. 8a), the simulated losses for sparsely populated municipalities in the Bernese

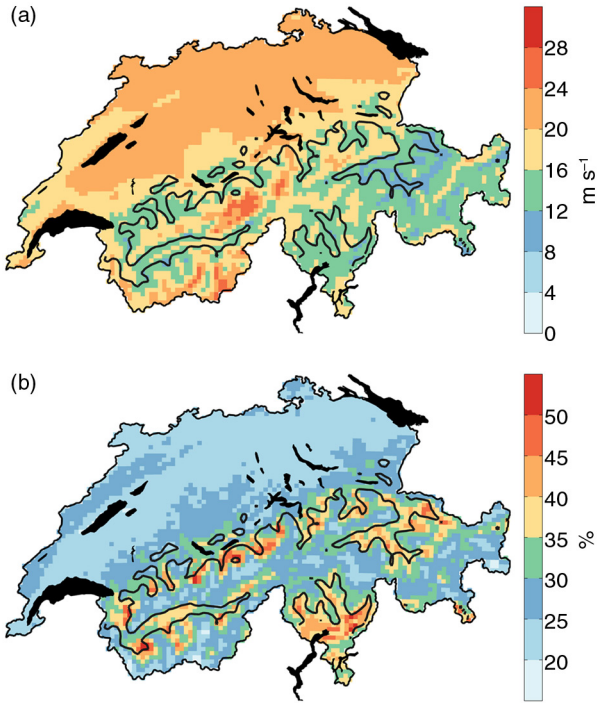

Fig. 8. (a) Composite mean of the wind gust footprints for all 84 windstorm events in m s^{-1} (colour scheme). (b) Composite coefficient of variation in %; the composite coefficient of variation was calculated from the ratio of the composite standard deviation to the composite mean. The WRF terrain height 1500 m a.s.l. contour line and lakes are outlined.

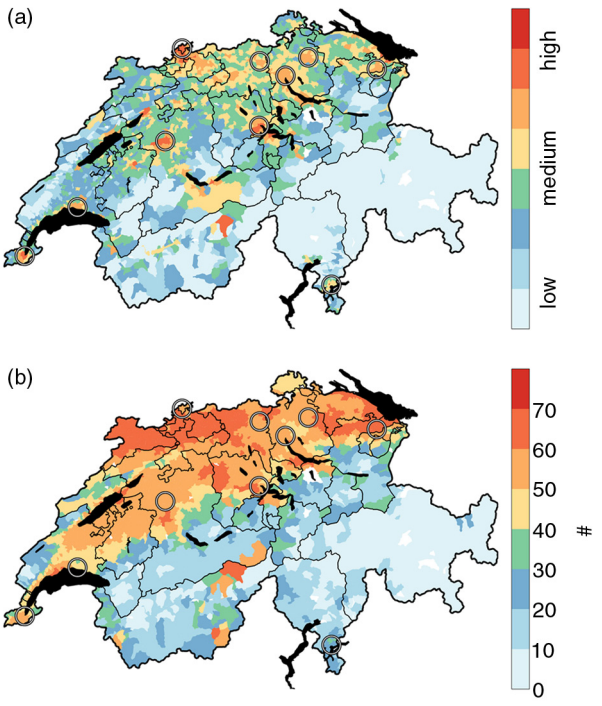

Fig. 9. (a) Composite mean of simulated loss per km^2 at municipal level for all 84 windstorm events (colour scheme; base 10 logarithmic scale). (b) For each municipality, number of windstorm events with simulated loss greater than zero (maximum number = 84 events). Circles indicate the 10 major agglomerations of Switzerland in 2009. Cantonal boundaries and lakes are outlined.

Oberland are high on average (Fig. 9a). To investigate whether the composited loss values are due to few severe windstorm events or due to several weaker events, the loss event frequency at municipal level (i.e. number of windstorm events at municipal level with simulated loss greater than zero) is analysed in addition (Fig. 9b). The loss event frequency is highest for municipalities in the Swiss Plateau, partly for municipalities located in the Jura Mountains, and for high mountain regions like the Bernese Oberland and the Valais Alps.

As aforementioned, the advantage of downscaling the 20CR is that it spans a much longer time period than any other atmospheric reanalysis, which in most cases only span the period since about the 1950s (note that the novel 20CR version V2c covers 1851–2012). To examine the additional information from considering the full available period of 140 yr (1871–2011) compared to considering the period since 1950 only, wind gust speed and loss composites for the two sub-periods 1871–1949 (43 windstorm events) and 1950–2011 (41 events) are shown in Fig. 10. The wind gust composite for 1871–1949 shows overall lower values than the composite for 1950–2011, with the largest wind gust speed differences over the Swiss Plateau (>3 m s^{-1} on average). Correspondingly, the loss composite for 1871–1949 shows overall lower values than the composite for 1950–2011, apart from a few municipalities located in the Alps and in the Jura Mountains. Overall, the loss composites for both sub-periods are similar concerning the spatial pattern of losses.

Figure 11 shows the simulated losses summed over all Swiss municipalities for each of the 84 windstorm events in 1871–2011. Applying a threshold of simulated losses of 1 million CHF gives 12 loss events in 1871–1949 and 18 events in 1950–2011. Thus, excluding the period before 1950 would involve losing information of 40 % of such hazardous windstorm events. Concerning the strongest windstorms, eight of the top 10 loss events occurred after 1950 (see also Table 3).

Both Figs. 10 and 11 indicate that with considering the full period 1871–2011 we gain additional information of the wind gust footprints and associated losses of the slightly weaker windstorms. Information that is important for the correct calculation of return periods of windstorm events for instance.

5. Discussion

Besides the great potentials of our loss modelling technique – for example, that we are able to realistically simulate the

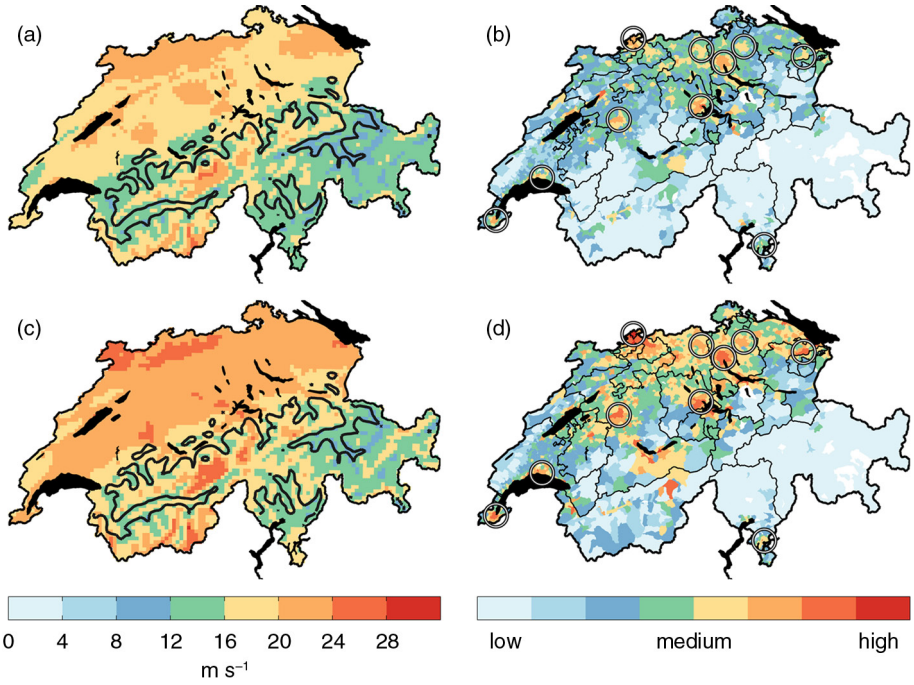

Fig. 10. (a, c) Composite mean of the wind gust footprints for the windstorm events in (a) 1871–1949 (43 events) and (c) 1950–2011 (41 events) in m s^{-1} (colour scheme). The WRF terrain height 1500 m a.s.l. contour line and lakes are outlined. (b, d) Composite mean of simulated loss per km^2 at municipal level for the windstorm events in (b) 1871–1949 and (d) 1950–2011 (colour scheme; base 10 logarithmic scale). Circles indicate the 10 major agglomerations of Switzerland in 2009. Cantonal boundaries and lakes are marked.

spatial patterns of windstorm losses – there are a number of uncertainties that need to be addressed. In this section, we discuss the main uncertainties of our approach in terms of the selection of windstorms, the dynamical downscaling and wind gust estimation, and the loss simulation technique.

5.1. *Selection of windstorms*

The windstorm events in our selection are not uniformly distributed over the period 1871–2011 (Fig. 11). Possible reasons could be decadal-scale variations of winter windstorms in Switzerland (Brönnimann et al., 2012; Welker and Martius 2014, 2015) as well as sampling issues. According to Stucki et al. (2014), all severe and extreme (in terms of damages) windstorm events that occurred in Switzerland since 1871 are included in the sample, but some moderately strong windstorms could be missing due to documentation discontinuities in space and time.

5.2. *Dynamical downscaling of the 20CR using WRF*

5.2.1. 20CR ensemble mean vs. ensemble members. For computational reasons, it was not possible to downscale each of the 56 20CR ensemble members for all 84 windstorm events, and therefore we downscaled the ensemble mean. In the

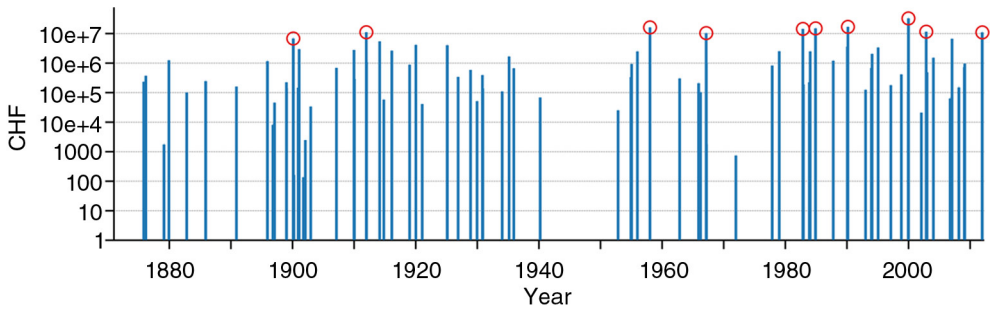

Fig. 11. Simulated loss summed over all Swiss municipalities in CHF for all 84 windstorm events under year-2009 asset distribution (blue bars; base 10 logarithmic scale; see also Supplementary Table A1). The top 10 windstorm events are marked with red circles (Table 3).

Table 3. The top 10 windstorm events in Switzerland during the winter months October through March of 1871–2011 concerning simulated loss summed over all Swiss municipalities

Rank	Date	Percentage loss	Windstorm name
1	1999-12-26	100.0	'Lothar'
2	1990-02-27	51.9	'Vivian'
3	1958-01-07	49.9	–
4	1984-11-23	46.1	–
5	1982-11-08	44.3	'Once-in-a-century' foehn storm
6	2002-11-15	35.8	'Uschi'
7	1911-12-22	34.1	–
8	2011-12-17	33.8	'Joachim'
9	1967-02-23	31.9	'Adolph-Bermpohl' windstorm
10	1900-02-14	20.9	–

Given is the date of the maximum downscaled surface wind gust speed over Switzerland during the respective event and the simulated loss for each event summed over all Swiss municipalities; expressed as a percentage of the simulated loss associated with 'Lothar' on 26 December 1999 (rank 1). If available/known, the name of the windstorm (associated low-pressure system) is given.

assimilation scheme of 20CR, an update is first computed for the ensemble mean, then the deviations from the ensemble mean are updated (Compo et al., 2011). The 20CR ensemble mean update can therefore be considered physically consistent (although this does not guarantee that the ensemble mean is always realistic when compared to real-world situations).

Downscaling the ensemble mean is a possible shortcoming of our approach since the ensemble mean is an average and hence a smoothed representation of the atmospheric conditions in the individual ensemble members. The effect on the downscaled surface winds and thus on the simulated losses is expected to be largest for historic events because the ensemble mean is biased towards lower wind speeds early in the record (Brönnimann et al., 2012); that is, in the period before about 1950, when the number of assimilated surface pressure and mean sea level pressure observations was considerably smaller than afterwards. Indeed, some historic windstorm events in our sample are probably too weak in our simulations: for example, the windstorm on 20 February 1879, classified as extreme in the windstorm catalogue of Stucki et al. (2014), only ranks 78th in our list of 84 events (Supplementary Table A1).

In mitigation, we note that the change in the 20CR ensemble range of the integrated winter wind loss potential in Switzerland is small compared to the interannual and decadal-scale variability (Welker and Martius, 2014). But how are individual historic windstorm events represented in the 20CR ensemble dataset? Stucki et al. (2015) showed that for the foehn storm in Switzerland in February 1925 (also included in our windstorm sample; rank 14 in Supplementary Table A1) the 20CR ensemble mean is a suitable estimate of the atmospheric conditions because most of the ensemble members are consistent with the ensemble mean in case of this specific windstorm event.

Furthermore, Stucki et al. (2016) analysed the 20CR ensemble range compared to the ensemble mean using the examples of two present windstorms in Switzerland (a foehn storm on 8 November 1982 and 'Lothar' on 26 December 1999) and two historic events (a foehn storm on 5 January 1919 and a westerly windstorm on 23 February 1935). All of these windstorm events are included in our windstorm sample (Supplementary Table A1); in terms of simulated losses, the two present events rank 5th (November 1982) and 1st (December 1999), and the two historic ones rank 33rd (January 1919) and 24th (February 1935). For all four windstorm events, the agreement among the 56 20CR ensemble members is good concerning the positions of the surface cyclone fields (and corresponding mean sea level pressure minima) over Europe associated with the high wind events in Switzerland (Stucki et al., 2016). The 20CR ensemble range, concerning the position and intensity of the surface cyclones, is slightly larger in case of the two historic windstorm events compared to the more recent ones. The same applies to the ensemble range of the near-surface wind speed for the Switzerland grid cells.

To examine whether the simulated loss patterns are strongly affected by our simplified approach of downscaling the 20CR ensemble mean instead of downscaling the ensemble members individually, we simulated losses based on downscaled wind gust fields from each ensemble member for both a historic westerly windstorm event and a present-day event, that is, for the aforementioned windstorm in February 1935 (see also Brönnimann et al., 2014) and for 'Lothar'. Then, we computed the ensemble maximum wind gust speed (loss) at every grid point (municipality) for both windstorms. This ensemble maximum approach gives the maximum expected wind gust speed (loss) at every grid point (municipality) if all ensemble members are taken into account. However, physical consistency of the resulting wind gust and loss patterns is not given anymore.

Figure 12 shows the comparison of the wind gust and loss patterns obtained by the ensemble maximum approach with the corresponding wind gust and loss patterns obtained by the ensemble mean approach (i.e. downscaling of the ensemble mean) for both windstorm events. For 'Lothar', the absolute differences between the two approaches regarding wind gust speed are smallest for the Swiss Plateau (approximately 5 m s^{-1} and smaller) and largest for southern Switzerland and parts of the Alps, where the ensemble maximum approach yields considerably higher values (in patches up to 15 m s^{-1}; Fig. 12c); the root-mean squared error (RMSE) for the whole of Switzerland is 4 m s^{-1}. The losses associated with the two approaches are overall similar for the Alps (Fig. 12d), even though the wind gust differences are largest there. However, wind gust speeds from both approaches are generally too low (mostly <30 m s^{-1}) to cause damage according to the damage function applied (the product of *MDD* and *PAA* is $<1.2{\cdot}10^{-5}$ for wind gusts <30 m s^{-1}; Fig. 3) and the values at risk are overall lower than in other regions of Switzerland (Fig. 2). Differences are larger for some municipalities located in the Jura Mountains and in the Swiss Plateau. The RMSE for the whole of Switzerland is 2741 CHF km^{-2}. Summed over all Swiss municipalities, the simulated loss for the ensemble maximum approach is increased by a factor of 1.3 compared to the ensemble mean approach. Thus, even if the simulated losses are overall higher in case of the ensemble maximum approach, the simulated losses are still much too low compared to the insurance loss data (see Section 3.3).

For the windstorm event in February 1935, the ensemble maximum approach gives higher wind gust speeds than the ensemble mean approach for most parts of Switzerland, with the largest absolute differences over the Alps (in patches over 15 m s^{-1}; Fig. 12a); the RMSE for the whole of Switzerland is 3.7 m s^{-1}. The loss differences are largest over the Swiss Plateau, where most of the assets are located, but differences are generally low (Fig. 12b). The RMSE for the whole of Switzerland is 337 CHF km^{-2}. Summed over all Swiss municipalities, the simulated loss is increased by a factor of 1.6 using the ensemble maximum approach compared to the ensemble mean approach. This factor is slightly higher compared to 'Lothar' (factor of 1.3; see above). For both the historic windstorm in 1935 and the present-day windstorm 'Lothar', the factors are relatively low still. Regarding windstorm losses, the additional information that we gain from downscaling all ensemble members individually is limited (bearing in

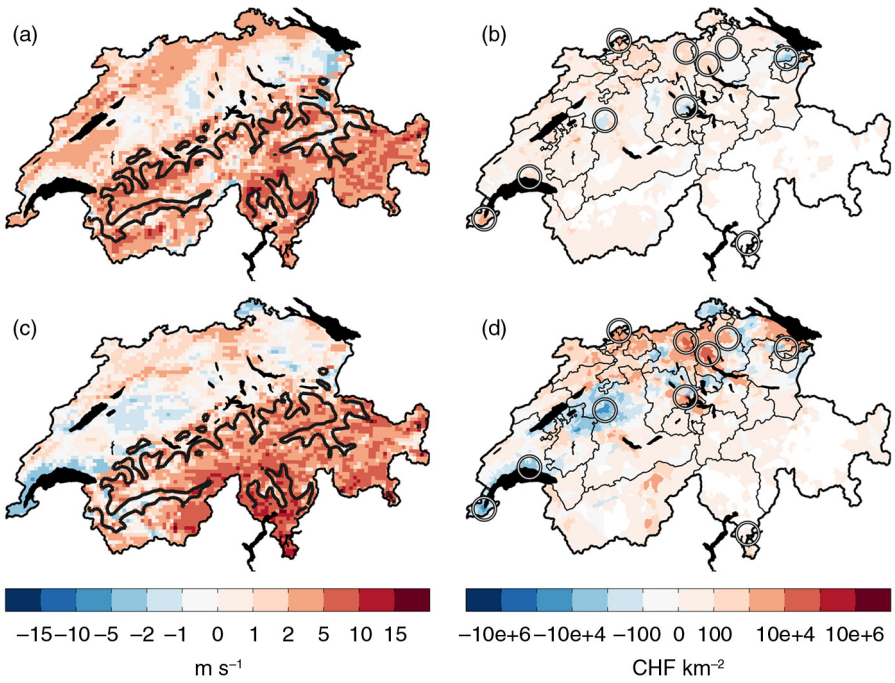

Fig. 12. The wind gust footprints for (a) the windstorm in February 1935 and (c) 'Lothar' were calculated first, based on (i) the ensemble mean approach and (ii) the ensemble maximum approach (see text for explanations), and the difference (ii) – (i) was computed subsequently (in m s^{-1}; non-linear colour scheme). The WRF terrain height 1500 m a.s.l. contour line and lakes are outlined. (b, d) Analogous to (a, c), but shown are the differences between the corresponding simulated losses in CHF per km^2 at municipal level under year-2009 asset distribution for the two approaches (colour scheme; base 10 logarithmic scale). Circles indicate the 10 major agglomerations of Switzerland in 2009. Cantonal boundaries and lakes are outlined.

mind that this inference is based on the results for two windstorms only).

Whereas the RMSE values for wind gust speed are on similar levels for both windstorm events (4 m s^{-1} vs. 3.7 m s^{-1}), the RMSE values for simulated loss differ more strongly (2741 CHF km^{-2} vs. 337 CHF km^{-2}). This, in turn, illustrates that changes in wind gust speed lead to larger changes in damages in case of very intense windstorm events such as 'Lothar' compared to weaker ones, owing to the non-linear relationship between wind gust speeds and inflicted damages.

5.2.2. Mean wind and wind gust estimation. The surface wind gust estimation methods applied in this study [eqs. (1–3)] basically combine the mean (sustained) surface wind speed and a fluctuating component that has to be parameterised. Thus, errors in estimated surface wind gust speeds arise from the wind gust estimation method itself and from erroneous mean wind speeds (see Stucki et al., 2016).

For 'Lothar', the estimated surface wind gusts using both the WPD method and the COS method are systematically too low over the Swiss Plateau compared to instrumental wind gust speed measurements (Table 1). This indicates that the mean surface wind speeds, used in both wind gust estimations, are already too low for this region. Compared to the WPD method, the COS method generates higher wind gusts over high orography, but overall lower gusts in the Swiss Plateau and in deep Alpine valleys (Fig. 13a). Similar conclusions can be drawn for the other windstorm events in our sample (Fig. 13b). The comparison of instrumental wind gust speed measurements and estimated surface wind gust speeds shows that for 'Lothar' the WPD wind gust estimates are more accurate than the COS wind gusts for all stations regardless of their topographical location (Table 1). In case of 'Joachim', the performance of the WPD method is on average lower for mountain and valley locations, whereas the performance of the two methods is approximately equal for stations located in flat terrain (Table 1). Consequently, no wind gust estimation is superior in all situations (see also Stucki et al., 2016). Furthermore, the example of 'Lothar' suggests that it is important to consider biases in the downscaled mean wind, besides optimising the wind gust estimation method itself.

Figure 14 shows composites of the losses simulated based on the WPD method and on the COS method. Differences between the two loss composites are largest over high orography and smallest over the Swiss Plateau. Nevertheless, differences are partly large for certain regions of the Swiss Plateau, for example, for Zurich, the largest city in Switzerland. An important difference between the two loss composites is that metropolitan areas generally stand out less clearly in the loss composite using the COS wind gust estimation method compared to the loss composite using the WPD method. Latter could be due to the differences of the two methods in representing the spatial characteristics of the wind gust footprints, with the COS method representing more strongly smaller-scale features of the wind gust field influenced by the local orography and thus giving spatially more heterogeneous wind gust footprints than the WPD method. In summary, the simulated loss potentials of Swiss windstorms depend on the wind gust estimation method applied, in particular for regions characterised by high orography.

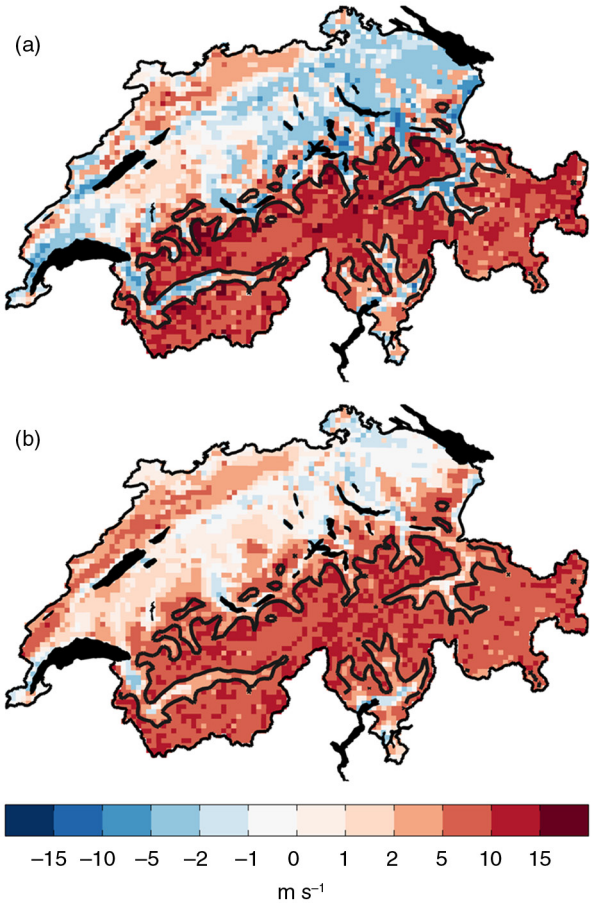

Fig. 13. (a) Differences between the wind gust footprint for 'Lothar' based on the COS wind gust estimation method and the wind gust footprint based on the WPD method in m s^{-1} (i.e. COS – WPD; non-linear colour scheme). (b) Analogous to (a), but shown is the difference between the wind gust speed composite mean for all 84 windstorm events using the COS method and the composite based on the WPD method. The WRF terrain height 1500 m a.s.l. contour line and lakes are outlined.

5.3. Simulation of windstorm-related economic losses

5.3.1. Vulnerability and asset distribution. A further source of uncertainty is that the vulnerability factors used

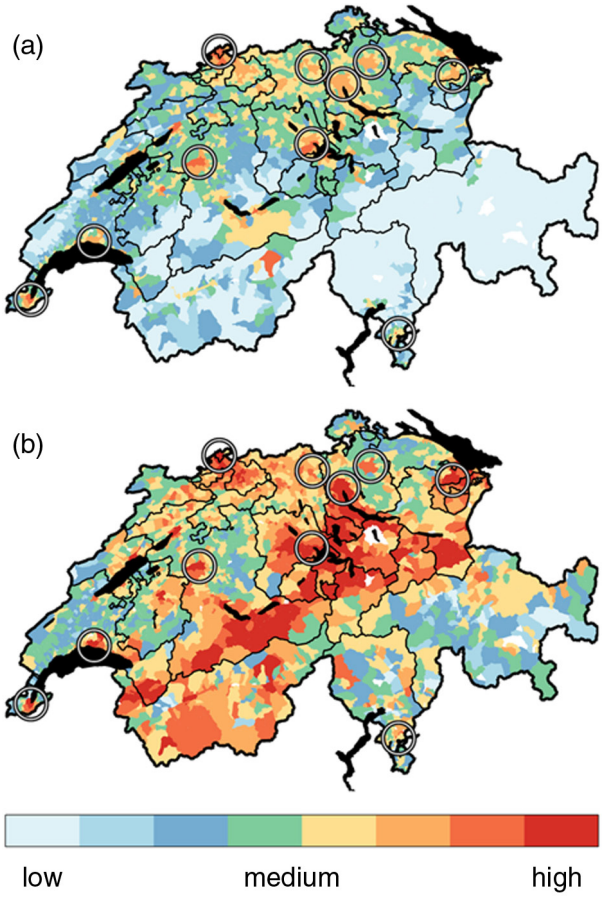

Fig. 14. Composite mean of simulated loss per km^2 at municipal level for all 84 windstorm events (colour scheme) using (a) the WPD wind gust estimation and (b) the COS wind gust estimation. Circles indicate the 10 major agglomerations of Switzerland in 2009. Cantonal boundaries and lakes are outlined. Figure 14a is the same as Fig. 9a.

in this study were determined based on windstorm loss data for the whole of Europe and on both movable property losses and building losses (Schwierz et al., 2010). Vulnerability factors determined for Swiss exposure only would be desirable and a distinction between movable properties and buildings (ideally further differentiating between building types) should be made in a future model setup. In addition, the vulnerability factors should ideally vary across Switzerland to capture the geographical heterogeneity of the susceptibility to damage. They could involve the adaption of buildings and infrastructure to local wind conditions; such adaptation measures are undertaken, for example, in valleys frequently exposed to high foehn winds.

Prescribing the present-day population distribution at municipal level and assuming assets of 250 000 CHF per inhabitant in the climada model is obviously an oversimplification and a more realistic distribution of values at risk would be desirable. More realistic data (at block or even single building resolution, indication of occupancy type, possibly even indication of construction type and/or quality) could, on the one hand, further enhance results; on the other hand, sparsity of detailed reported loss information etc. might render such an effort not worth undertaking. A balanced approach with respect to availability of data as followed in the present study yields robust results and only substantial additional efforts might further refine them.

5.3.2. Spatial association of hazard intensity to asset. In our current model setup, the wind gust speeds available on a latitude–longitude grid are associated with the assets at municipal level using the geographical centroids of the municipalities (see Section 2). This approach works well for municipalities in the Swiss Plateau. But the approach can be problematic for municipalities in the Alps or in the Jura Mountains, where assets are typically located at the valley bottoms but wind speeds are highest on the mountain tops. There, improvements of the loss simulation are to be expected if the geographical location of the municipality's main settlement is used instead of the geographical centroid of the municipality (note that information on the main settlement of each municipality was not available for the present study). Our approach of spatial association of hazard intensity to asset is more problematic for the simulation of losses based on the COS wind gust estimation method because the COS method tends to represent smaller-scale features of the wind gust field than the WPD method.

6. Summary and conclusions

We have applied the loss modelling approach presented by Stucki et al. (2015) to a sample of 84 high-impact winter windstorms that affected Switzerland between 1871 and 2011. This loss modelling technique involves the dynamical downscaling of the 20CR ensemble mean to a 3 km by 3 km horizontal grid over Switzerland using the WRF model. Wind gust fields estimated from the high-resolution simulations (using the WPD wind gust estimation method) have served as input for the simulation of economic windstorm losses in the climada model.

For our windstorm sample, we have calculated composites of both wind gust speed and simulated loss. In accordance with the wind gust speed composite, the composite of simulated loss in general reveals high values north of the Alps, in particular for the densely populated Swiss Plateau located in between the Jura Mountains and the Alps, and lower values for south-eastern Switzerland. Metropolitan areas stand out in the loss composite demonstrating that windstorm losses are related to the distribution of assets as well as to the distribution of hazardous winds.

The loss composite for all windstorm events in the subperiod 1871–1949 shows overall lower values than the composite for the windstorms in 1950–2011, apart from few municipalities situated in the Alps and in the Jura Mountains. Thus, with considering the full period since 1871, compared to considering the period since 1950 only, we obtain further information about the wind gust footprints and associated losses of the slightly weaker windstorms. This additional information is important for the correct calculation of return periods of windstorm events. Eight events out of the top 10 loss events (concerning simulated losses summed over all municipalities in Switzerland) occurred after 1950. This is affected by decadal-scale changes in the loss potentials of winter windstorms in Switzerland (see Welker and Martius 2014, 2015), windstorm sampling issues (Stucki et al., 2014), and our simplified approach of downscaling the 20CR ensemble mean instead of downscaling the ensemble members individually; the ensemble mean is biased towards lower wind speeds in the period before around 1950 (Brönnimann et al., 2012). To examine whether the simulated loss patterns are strongly affected by this simplified approach, we have performed additional loss simulations based on downscaled wind gust fields from each of the 56 20CR ensemble members for both a windstorm in February 1935 and for 'Lothar' in December 1999. These analyses have shown that the additional information, in terms of windstorm losses, that we gain from downscaling all ensemble members individually is limited (in view of the fact that this conclusion is based on two windstorm events only).

A comparison of simulated losses with insurance loss data for two present-day highly damaging winter windstorms in Switzerland ('Lothar' in December 1999 and 'Joachim' in December 2011) indicates that our loss simulation captures well the spatial pattern of the losses – confirming the promising results of Stucki et al. (2015) for a foehn storm in Switzerland in 1925. However, the loss amplitude is strongly underestimated for 'Lothar', while it is better simulated for 'Joachim'. In case of 'Joachim', insured losses are approximately three times as high as the simulated losses (in the non-GUSTAVO cantons), but 17 times as high in case of 'Lothar'. Our results suggest that this substantial underestimation of the loss amplitude in case of 'Lothar' is mainly due to an underestimation of the mean wind and hence the wind gusts over Switzerland: that is, negative wind gust speed bias of 7 m s^{-1} on average compared with instrumental wind gust measurements. Encouragingly, a simple correction of this wind gust speed bias results in an almost perfect simulation concerning the loss amplitude. The strong underestimation of the wind gusts (and associated losses) in case of 'Lothar' is not representative for other windstorm events in our sample (see also Stucki et al., 2016). For 'Joachim', the agreement of the estimated wind gust speeds over Switzerland with the instrumental wind gust measurements is very good (positive bias of 0.2 m s^{-1} on average), resulting in a much better simulation of the loss amplitude than in case of 'Lothar'. Our results emphasise the importance of an accurate estimation of the wind gust footprint for the loss simulation. Furthermore, wind gust speed biases are most relevant for the loss simulation in case of very intense windstorm events such as 'Lothar', due to the non-linear damage function applied. It is important to note that a full comparison between the simulated losses and the available insurance loss data is complicated by the characteristics of the available insurance data and by peculiarities of the Swiss insurance system.

The simulated losses are highly sensitive to relatively small changes in wind gust speed owing to the non-linear damage function applied (which is particularly the case for the strongest events; see also Watson and Johnson, 2004). Thus, uncertainties concerning the loss simulation arise from the wind gust estimation method applied because wind gust estimates differ in some areas considerably among the different estimation methods. In this study, we have compared two standard wind gust estimation methods, the WPD method and the rather complementary COS method. Differences between the simulated losses using the WPD method and the simulated losses using the COS method are generally largest over high orography such as the Alps and the Jura Mountains and smallest over the Swiss Plateau. Consequently, at least for insurance applications the large uncertainties associated with the selection of the wind gust estimation method might be less important because the uncertainties are generally lowest in the Swiss Plateau, where most of the values at risk are located. The dependency on the applied wind gust estimation method particularly concerns regions/countries characterised by a complex orography, where standard wind gust estimation methods encounter limits. Our results further indicate that no wind gust estimation method is superior in all situations (see also Stucki et al., 2016).

One possibility to obtain more realistic wind gust speeds for the loss simulation is to simply add biases depending on the respective wind gust estimation method and windstorm event. Bias corrections are particularly relevant for very intense windstorm events and the approach has proved to be suitable for 'Lothar'. Furthermore, the example of 'Lothar' has shown that it is important to also consider biases in the downscaled mean wind. Another possibility could be to empirically adapt the wind gust estimation methods by tuning the constant parameters in the estimation methods (e.g. in the COS method) for windstorms in Switzerland. A drawback of both possibilities is that observations of wind gust speeds at high spatiotemporal resolution are necessary, which are not always available.

Besides uncertainties associated with the simulation of the wind gust footprint itself, there are uncertainties associated with our assumptions regarding the exposure and vulnerability of the values at risk. Both the distribution of values at risk and the vulnerability factors (which are a function of wind gust speed) used in the current model setup are simplifications of reality. There remain many opportunities to improve the model to obtain a simulation of the loss amplitude that is appropriate for applications in the insurance industry for instance. Besides being able to simulate windstorm-related wind gust speeds as accurately as possible, we regard a further development/an adjustment of the damage function derived by Schwierz et al. (2010) as important (ideally, a damage function determined based on windstorm loss data for Switzerland only with a distinction between movable properties and buildings). Necessary to that end is a close collaboration between, on the one hand, the insurance industry making available information on insured values at risk and losses as well as vulnerabilities and, on the other hand, the scientific community providing information on the wind gust footprints of windstorms at high spatiotemporal resolution.

In conclusion, this study has shown that it is challenging to accurately simulate windstorm-related wind gusts and losses for Switzerland, with its very complex orography. Nonetheless, with the presented loss modelling technique we are able to realistically simulate the spatial patterns of losses associated with historic and present high-impact winter windstorms in Switzerland, and there in particular for regions in the Swiss Plateau that are characterised by a relatively flat orography. This spatial information on the losses is useful to many end-users involved in the assessment of windstorm risks. Not least, this study has shown that the evaluation of our loss modelling technique suffers from limitations of claims and exposure data. Thus, further evaluation and improvement of the methodology depend on collaborations and a mutual exchange of information between the scientific community and the insurance industry.

7. Acknowledgements

We are very thankful to the Swiss Mobiliar and the Intercantonal Reinsurance for providing insurance loss data. Support was provided by Meteotest, the Swiss Federal Office for the Environment, MeteoSwiss, and the Dr. Alfred Bretscher Fonds. Support for the Twentieth Century Reanalysis Project dataset is provided by the U.S. Department of Energy, Office of Science Innovative and Novel Computational Impact on Theory and Experiment (DOE INCITE) program, and Office of Biological and Environmental Research (BER), and the National Oceanic and Atmospheric Administration Climate Program Office.

References

Bresch, D. N. 2014. Climada model code, windstorm module and documentary material. Online at: https://github.com/davidnbresch/climada, https://github.com/davidnbresch/climada_module_ws_europe, http://www.iac.ethz.ch/edu/courses/master/modules/climate-risk.html

Brönnimann, S., Martius, O. and Dierer, S. 2014. Die Wetter-Zeitmaschine. *Phys. Unserer. Zeit*. **45**, 84–89.

Brönnimann, S., Martius, O., von Waldow, H., Welker, C., Luterbacher, J. and co-authors. 2012. Extreme winds at northern mid-latitudes since 1871. *Meteorol. Z.* **21**, 13–27.

Compo, G. P., Whitaker, J. S., Sardeshmukh, P. D., Matsui, N., Allan, R. J. and co-authors. 2011. The Twentieth Century Reanalysis project. *Q. J. Roy. Meteorol. Soc.* **137**, 1–28.

Della-Marta, P. M., Liniger, M. A., Appenzeller, C., Bresch, D. N., Köllner-Heck, P. and co-authors. 2010. Improved estimates of the European winter windstorm climate and the risk of reinsurance loss using climate model data. *J. Appl. Meteorol. Climatol.* **49**, 2092–2120.

Economics of Climate Adaptation Working Group (ECAWG). 2009. Shaping climate-resilient development: a framework for decision-making. Report by ClimateWorks Foundation, Global Environmental Facility, European Commission, McKinsey & Company, The Rockefeller Foundation, Standard Chartered Bank and Swiss Re. Online at: http://media.swissre.com/documents/rethinking_shaping_climate_resilent_development_en.pdf

Federal Office for the Environment (FOEN). 2015. Wind hazard map for Switzerland. Online at: https://map.geo.admin.ch

Frei, C. and Schär, C. 2001. Detection probability of trends in rare events: theory and application to heavy precipitation in the alpine region. *J. Clim.* **14**, 1568–1584.

Haas, R. and Pinto, J. G. 2012. A combined statistical and dynamical approach for downscaling large-scale footprints of European windstorms. *Geophys. Res. Lett.* **39**, L23804.

Haylock, M. R. 2011. European extra-tropical storm damage risk from a multi-model ensemble of dynamically-downscaled global climate models. *Nat. Hazards. Earth. Syst. Sci.* **11**, 2847–2857.

Imhof, M. 2011. Analyse langfristiger Gebäudeschadendaten. Interkantonaler Rückversicherungsverband IRV.

IPCC. 2012. Managing the risks of extreme events and disasters to advance climate change adaptation. In: *A Special Report of Working Groups I and II of the Intergovernmental Panel on Climate Change* (eds. C. B. Field, V. Barros, T. F. Stocker, D. Qin, D. J. Dokken, K. L. Ebi and co-editors). Cambridge University Press, Cambridge, UK, p. 582.

Jungo, P., Goyette, S. and Beniston, M. 2002. Daily wind gust speed probabilities over Switzerland according to three types of synoptic circulation. *Int. J. Climatol.* **22**, 485–499.

Keiler, M., Sailer, R., Jörg, P., Weber, C., Fuchs, S. and co-authors. 2006. Avalanche risk assessment – a multi-temporal approach, results from Galtür, Austria. *Nat. Hazards. Earth. Syst. Sci.* **6**, 637–651.

Klawa, M. and Ulbrich, U. 2003. A model for the estimation of storm losses and the identification of severe winter storms in Germany. *Nat. Hazards. Earth. Syst. Sci.* **3**, 725–732.

Raible, C. C., Kleppek, S., Wüest, M., Bresch, D. N., Kitoh, A. and co-authors. 2012. Atlantic hurricanes and associated insurance loss potentials in future climate scenarios: limitations of high-resolution AGCM simulations. *Tellus A* **64**, 15672. DOI: http://dx.doi.org/10.3402/tellusa.v64i0.15672

Reguero, B. G., Bresch, D. N., Beck, M. W., Calil, J. and Meliane, I. 2014. Coastal risks, nature-based defenses and the economics of adaptation: an application in the Gulf of Mexico, USA. *Coast. Eng. Pro.* **1**, management.25. DOI: http://dx.doi.org/10.9753/icce.v34.management.25

Richner, H. and Hächler, P. 2013. Understanding and forecasting Alpine foehn. In: *Mountain Weather Research and Forecasting, Chapter 4* (eds. F. K. Chow, S. F. J. De Wekker and B. J. Snyder). Springer Atmospheric Sciences, Dordrecht, The Netherlands, pp. 219–260. DOI: http://dx.doi.org/10.1007/978-94-007-4098-3_4

Schulz, J.-P. 2008. Revision of the turbulent gust diagnostics in the COSMO model. *COSMO Newslett.* **8**, 17–22.

Schulz, J.-P. and Heise, E. 2003. A new scheme for diagnosing near-surface convective gusts. *COSMO Newslett.* **3**, 221–225.

Schwierz, C., Köllner-Heck, P., Zenklusen Mutter, E., Bresch, D. N., Vidale, P.-L. and co-authors. 2010. Modelling European winter wind storm losses in current and future climate. *Clim. Change.* **101**, 485–514.

Skamarock, W. C., Klemp, J. B., Dudhia, J., Gill, D. O., Barker, D. M. and co-authors. 2008. *A Description of the Advanced Research WRF Version 3*. Tech. Note 475 + STR, National Center for Atmospheric Research, Boulder, CO, 113 pp.

Stucki, P., Brönnimann, S., Martius, O., Welker, C., Imhof, M. and co-authors. 2014. A catalog of high-impact windstorms in Switzerland since 1859. *Nat. Hazards. Earth. Syst. Sci.* **14**, 2867–2882.

Stucki, P., Brönnimann, S., Martius, O., Welker, C., Rickli, R. and co-authors. 2015. Dynamical downscaling and loss modeling for the reconstruction of historical weather extremes and their impacts – a severe foehn storm in 1925. *Bull. Am. Meteorol. Soc.* **96**, 1233–1241. DOI: http://dx.doi.org/10.1175/BAMS-D-14-00041.121

Stucki, P., Dierer, S., Welker, C., Gómez-Navarro, J. J., Raible, C. C. and co-authors. 2016. Evaluation of wind gust parameterizations for recent and historical windstorms in Switzerland. *Tellus A*.

Watson, C. C., Jr. and Johnson, M. E. 2004. Hurricane loss estimation models: opportunities for improving the state of the art. *Bull. Am. Meteorol. Soc.* **85**, 1713–1726.

Welker, C. and Martius, O. 2014. Decadal-scale variability in hazardous winds in northern Switzerland since end of the 19th century. *Atmos. Sci. Lett.* **15**, 86–91.

Welker, C. and Martius, O. 2015. Large-scale atmospheric flow conditions and sea surface temperatures associated with hazardous winds in Switzerland. *Clim. Dynam.* **44**, 1857–1869.

Wernli, H., Dirren, S., Liniger, M. A. and Zillig, M. 2002. Dynamical aspects of the life cycle of the winter storm 'Lothar' (24-26 December 1999). *Q. J. Roy. Meteorol. Soc.* **128**, 405–429.